Separation Science and Technology
Publication details, including instructions for authors and subscription information:
http://www.informaworld.com/smpp/title~content=t713708471

Physicochemical Factors Influencing Colloidal Particle Transport in Porous Media

Sung-Jae Kim[a]; Larry D. Benefield[b]
[a] DEPARTMENT OF FOOD SCIENCE FISHERIES COLLEGE GYEONGSANG, NATIONAL UNIVERSITY, GYEONGNAM, SOUTH KOREA [b] DEPARTMENT OF CIVIL ENGINEERING, AUBURN UNIVERSITY, AUBURN, ALABAMA, USA

To cite this Article Kim, Sung-Jae and Benefield, Larry D.(1996) 'Physicochemical Factors Influencing Colloidal Particle Transport in Porous Media', Separation Science and Technology, 31: 19, 2621 — 2653
To link to this Article: DOI: 10.1080/01496399608000817
URL: http://dx.doi.org/10.1080/01496399608000817

SEPARATION SCIENCE AND TECHNOLOGY, 31(19), pp. 2621–2653, 1996

Physicochemical Factors Influencing Colloidal Particle Transport in Porous Media

SUNG-JAE KIM
DEPARTMENT OF FOOD SCIENCE
FISHERIES COLLEGE
GYEONGSANG NATIONAL UNIVERSITY
445 INPYEONG-DONG, TONGYEONG, GYEONGNAM, SOUTH KOREA 650-160

LARRY D. BENEFIELD
DEPARTMENT OF CIVIL ENGINEERING
AUBURN UNIVERSITY
AUBURN, ALABAMA 36849, USA

ABSTRACT

The mobilization/immobilization of colloidal-sized particles which have high surface areas per unit mass is an important process occurring in groundwater flow systems. Association of contaminants with mobile colloidal particles may enhance the transport of adsorbed pollutants, or deposition of colloidal particles in porous media may decrease permeability and reduce contaminant transport. The general objective of this work was to elucidate physical and chemical factors affecting colloidal particle (Brownian and non-Brownian) transport in porous media under typical groundwater flow velocities. The most critical chemical factor influencing Brownian particle (0.1 and 1.0 μm) transport in a packed column was found to be pH. The next most critical factor was electrolyte concentration (calcium ion and sodium ion concentration). Gravitational force was found to be an important factor for non-Brownian particle (10 μm) transport. The non-Brownian particle transport was observed to be independent of solution chemistry. Increases in superficial velocity (from 0.9 to 2.7 m/day) resulted in different types of behavior for Brownian and non-Brownian particle transport under different conditions. The Brownian particle throughputs at a superficial velocity of 0.9 m/day were mainly controlled by the surface interaction forces, that is, hydrodynamic action was not important. The difference in Brownian diffusivity between 0.1 and 1.0 μm particles caused opposite results in particle throughputs in all experimental columns regardless of solution chemistries. Particles of 0.1 μm produced the maximum transport

in the column filled with the smallest glass beads, while 1.0 μm particles produced the maximum transport in the column packed with the largest glass beads.

INTRODUCTION

Problem Statement and Significance

The transport of suspended particles may be an important process occurring in groundwater flow systems. The fate of many pollutants in the aquatic environment is determined by the fate of the particulate matter with which they are associated. The transport of hydrophobic organics and toxic metals depends on the degree of partitioning of these compounds between solution and solid phases. Traditionally, contaminants in a groundwater system have been viewed as occurring in two phases such as dissolved in water and hence mobile, and sorbed to or precipitated on solids and, therefore, stationary. This conceptualization disregards a contaminant association with a potentially important third phase, the colloids, which, in relation to the other two phases, may be characterized as mobile solids. Examples include viruses, bacteria, Giardia cysts, asbestos fibers, radionuclides, heavy metals, and synthetic organics adsorbed to the surface of mineral and detrital particles. In all cases the suspended particles of most concern with regard to transport potential are in the colloidal size range (micrometer and submicrometer). These small particles have high surface areas per unit mass, thus posing a significant sorption potential. Since they are considerably smaller than sands and gravels encountered in groundwater aquifers, migration of compounds associated with the suspended solid phase may occur, a process as yet not adequately considered in predictive models of contaminant migration. In the past the effect of colloidal material on the transport of contaminants in groundwater has largely been ignored because of poor methods of isolation, detection, and characterization. However, instrumentation has improved during the past few years and interest in this area of research has begun to intensify.

There is ample evidence that colloidal-sized particles can move in aquifers. When colloidal kaolin particles were given a negative charge by sorbing phosphate, Champlin (1) observed that they could move through laboratory columns filled with sand. Nightingale and Bianchi (2) determined that colloidal clay particles mobilized from surface soils were responsible for turbidity observed in wells several hundred meters from the recharge site. Robertson et al. (3) demonstrated that organic macromolecules can be transported by groundwater when they observed tannins and lignins more than 1000 m from a waste pulp liquor lagoon.

Aside from the evidence of colloid mobility, there is evidence that contaminants such as heavy metals, radionuclides, and hydrophobic organic compounds can sorb to the surface of colloidal-sized particles. The composition of colloidal particles is chemically similar to clay and metal oxide surfaces or the organic coating of immobile aquifer material. These colloidal particles can sorb organic and inorganic contaminants and stabilize them in the mobile phase. Association of contaminants with mobile colloidal particles may enhance the transport of highly adsorbed pollutants, or deposition of colloidal particles in porous media may decrease permeability and reduce contaminant transport.

It is recognized that bacteria and viruses can travel considerable distances in aquifers and saturated soils, thus posing a contamination threat to surface waters and well waters (4). A large number of outbreaks of water-borne disease have been attributed to contaminated groundwater (5). Reviews by Keswick and Gerba (6) and Gerba and Goyal (7) report bacterial migration up to 800 m and virus migration up to 400 m from their source.

The transport described above may have been governed by both hydrodynamic actions and surface interaction forces between particles and collector. However, there have been few research efforts within such a framework. Recently McDowell-Boyer et al. (8) and Corapcioglu and Haridas (9, 10) reviewed particle transport in groundwater systems and included extensions of filtration theories. Thus, the work described in this paper was undertaken to extend our current understanding of the factors (physical and chemical) governing colloidal particle transport in porous media.

The mechanisms of colloidal particle transport in subsurfaces are often based on those of colloidal particle transport in deep bed filtration. In deep bed filtration, particles are removed from the flowing suspension and deposited on the surface of the grains or fibers which comprise the porous filter media. Pore sizes are much larger than the suspended particle size so that removal by straining or sieving by the filter media or cake of deposited particles is not a dominant removal mechanism in the deep bed filtration process. However, removal by physical-chemical forces is a dominant mechanism in the process.

The fundamental mechanisms that are considered in evaluating the effects of chemistry on particle deposition in porous media have wide application and significance in natural and engineered systems that involve solid–liquid separation. Some examples include the coagulation of suspensions to achieve particle growth, the dewatering of sludges, the swelling properties of clays, and in general the fate of particle reactive pollutants in natural waters. Improved understanding in one area will have concomitant beneficial effects for research in other areas as well.

Objectives and Scope of Work

The primary purpose of this work was to extend our current understanding of the factors (physical and chemical) that influence the transport of colloidal particle through porous media. The scope of work was restricted to model or ideal systems. The work was also restricted to examining the particle transport in clean packed columns.

The experimental work involved using spherical glass bead collectors (0.105 to 0.15, 0.25 to 0.3, and 0.5 to 0.75 mm in size), spherical synthetic latex (polystyrene) suspended particles (0.1, 1.0, and 10 μm in size), relatively simple solution chemistry (NaCl and $CaCl_2$ electrolytes, and pH), and typical groundwater flow velocities (0.9 and 2.7 m/day). Particle transport experiments were carried out in clean packed columns of glass beads with independent variation of collector size, flow velocity, and solution chemistry. The "system chemistry" encompasses the bulk solution chemistry (concentration and type of dissolved ions and molecules) and the intrinsic surface chemistry of the suspended particles and the porous media (material type, nature of surface charge, type of surface chemical groups).

This model system approach was based on the premise that the elucidation of fundamental processes in such systems will ultimately improve understanding of the factors which influence the mobilization/immobilization of colloidal particles in the subsurface environment in relation to the properties of the subsurface media.

PHYSICAL AND CHEMICAL FILTRATION THEORIES

Colloidal particle transport in groundwater systems can be analyzed from a filtration perspective. Recently McDowell-Boyer et al. (8) and Corapcioglu and Haridas (9, 10) reviewed particle transport in groundwater systems and included extensions of filtration theories. Deep bed filtration is one example of particle transport with low Reynolds number flows occurring in a process in which a fluid suspension with low particle concentrations is passed through a filter composed of granular or fibrous media. The present study is focused on physical and chemical aspects of colloidal particle transport in the initial stages of porous media.

The fundamental mechanisms of interception (fluid drag), sedimentation, and Brownian diffusion for particle transport to an isolated spherical collector in uniform laminar flow as illustrated by Yao (11) are shown in Fig. 1. Interception is the result of the constriction of streamlines near the collector surface where the fluid velocity decreases because of a no-slip boundary condition that cause velocity gradients to occur in the fluid.

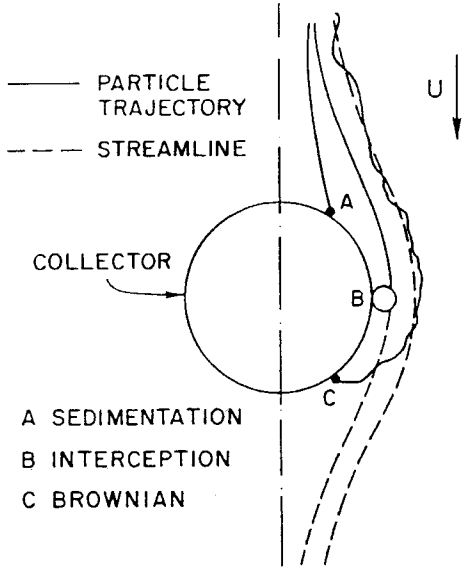

FIG. 1 Mechanisms of particle transport to an isolated spherical collector [after Yao (11)].

Hydrodynamic retardation and London–van der Waals (LVDW) attractive force are ignored in interception (11). Sedimentation can be predicted by calculating the rate at which particles settle onto the collector, assuming that all collisions result in sticking. The parameter controlling sedimentation is the Stokes settling velocity of the spherical particle (11). Submicron particles undergo random Brownian motion by bombardment of the particle by molecules of water, which promotes their deposition from suspensions flowing past spherical collectors. For a particle greater than about 1.0 μm in diameter, the viscous drag and inertia of the particle restrict the Brownian movement, and the mean free path (the mean magnitude of a random movement due to Brownian motion) of the particle is at most one or two particle diameters, and hence Brownian movement is not important. For a particle less than 1.0 μm, particle motion by this mechanism is stochastic in nature and becomes increasingly significant with decreasing sizes. Smaller particles are collected more efficiently due to their greater Brownian motion, assuming there is no repulsive energy barrier (12).

The collection of submicron particles (≤ca. 1.0 μm) under convection and Brownian diffusion can be modeled by solving the complete transport

equation under appropriate boundary conditions which take into account surface interactions through electrical double-layer (EDL) repulsion and LVDW attraction. When the surface interaction potentials have a large repulsive barrier and a low secondary minimum, the convective and the other transport terms of the diffusion equation may be conveniently omitted because under these conditions only diffusion and surface interactions are significant (13). In this case the collector surface appears as a sink which constantly consumes the arriving particles by an apparent first-order chemical reaction. This is called the surface interaction force boundary layer (SIFBL) approach (13–16). On the other hand, in the absence of EDL repulsion, no maximum in the interaction potential is expected. This suggests that the effects of the particle–collector interaction cannot be lumped into the SIFBL. In this case, LVDW attraction and hydrodynamic retardation are important only when they are sufficiently long-range to be coupled with convective diffusion, and the particle transport to the collector surface is mainly determined by the peclet number (14).

The deposition rate of non-Brownian particles ($\geq$ca. 1.0 μm) in a deep bed filter is dependent upon a number of dimensionless groups which characterize the various forces acting on the particle. For example, the Happel's sphere-in-cell flow model (16, 17) accounts for the presence of neighboring collectors by considering that the packed bed can be modeled using the trajectory approach by a single sphere encircled by a spherical liquid envelope. The dimensionless parameters associated with the trajectory analysis are shown in Table 1 with brief descriptions (16). Effects of various dimensionless groups on the total single collector efficiency are shown in Fig. 2 (18).

In Fig. 2, N_x denotes various surface interaction parameters. The EDL repulsive force may be quantified by N_{E1} based on ζ-potential. The dimensionless group, N_{E2} determines whether the double-layer interaction is attractive (nonpositive values of N_{E2}) or repulsive (positive N_{E2}). N_{DL} represents the magnitude of ionic strength and N_{Lo} is a London group that describes the LVDW attractive force varied by the Hamaker constant and particle size. The value of N_{Rtd} is proportional to the particle size but is inversely related to the distance between the particle and collector. N_{Rtd} is negligible at low values of N_{Lo} (or equivalently, the Hamaker constant) (18).

For small values of N_G (i.e., $\rho_p \approx \rho_f$, where ρ_p and ρ_f are densities of fluid and suspended particle, respectively), the gravitational force exerted on the particle is of comparable magnitude to the hydrodynamic force far from the wall and, therefore, a small change in the value of N_G results in a considerable change in the location of the limiting trajectory far from the immediate vicinity of the wall (19). For large values of N_G ($\geq 10^{-4}$),

TABLE 1
Various Dimensionless Parameters of the Trajectory Equation, their Definition and Ranges of Values

Parameters	Definition	Range of values
N_{DL}	κa_p Double layer group; dimensionless double-layer thickness, where κ is the inverse of the diffuse layer thickness and a_p is the radius of suspended particles	10 to 10^5
N_G	$2a_p^2(\rho_p - \rho_f)\, g/(9\mu U)$ Gravity group; dimensionless settling velocity of the particle, where ρ_p and ρ_f are the density of suspended particle and fluid, respectively, μ is the absolute viscosity of the solution, g is the gravitational acceleration, and U is the superficial velocity	-10^{-2} to 10^0
N_{RS}	a_p/a_c Relative size group; aspect ratio, where a_c is the radius of collector	10^{-4} to 10^{-1}
N_{Lo}	$A/9\pi\mu a_p^2 U$ London group, where A is the Hamaker constant	10^{-5} to 10^{-2}
N_{E1}	$\epsilon\kappa(\zeta_c^2 + \zeta_p^2)/(12\pi\mu U)$ Electrokinetic group 1, where ϵ is the electric permittivity of the solution and ζ_c and ζ_p are the zeta potential of collector and particles, respectively	10^{-1} to 10^3
N_{E2}	$2\zeta_c\zeta_p/(\zeta_c^2 + \zeta_p^2)$ Electrokinetic group 2; electrokinetic "parity" group	-1 to $+1$
N_{Rtd}	a_p/γ Retardation group; accounts for electromagnetic retardation of the London force, where γ is the characteristic wavelength for the interaction	10^0 to 10^3

however, the gravitational force dominates the hydrodynamic force, and, thus, the part of the limiting trajectory far from the immediate vicinity of the wall is almost parallel to the direction of gravity and changes little even for large increases of the N_G value. In this case the efficiency has a first-order dependence on N_G, thereby suggesting that the efficiency due to sedimentation alone is approximately equal to N_G (19, 20).

An increase in the value of the a_p/a_c (particle radius/collector radius) ratio leads to an increase in the value of N_{RS}. In this case particle collec-

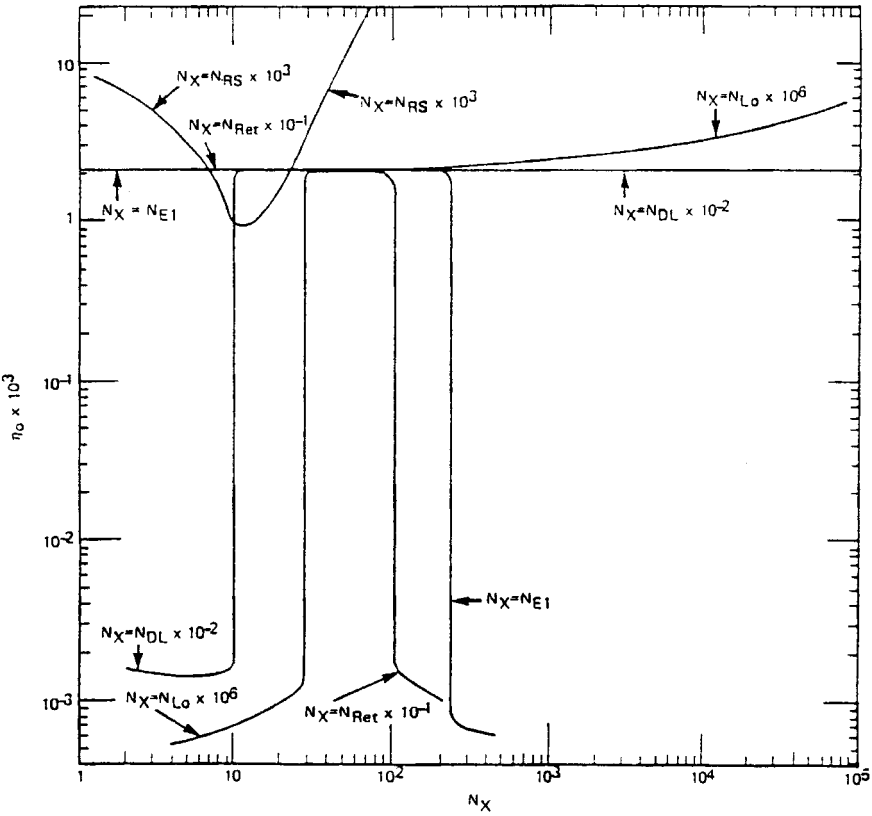

FIG. 2 Effects of various dimensionless groups (surface interaction parameters) on the total single collector efficiency. N_X is various dimensionless groups [after Tien (18)].

tion by interception also increases after passing through a minimum (i.e., the efficiency vs N_{RS} curve passes through a minimum point as shown in Fig. 2).

The surface interaction forces are determined by the LVDW, EDL, and hydrodynamic retardation. In general, the surface interactions are not important insofar as their net effect is attractive in the vicinity of the collector. However, when the EDL repulsive force exceed the LVDW attraction as a result of how the dimensionless groups vary, the EDL repulsion may dominate the gravitational and hydrodynamic forces in the immediate neighborhood of the collector. In Fig. 2 the low part of the collector efficiency values for each one of the dimensionless groups corre-

sponds to such cases. In fact, even when $N_{E2} < 0$, there is no enhancement of collection. The high efficiency value segment for each of these groups corresponds to the case when the EDL force is negligible at all separations between the particle and collector while at certain values of the EDL force the value of the efficiency may change very suddenly. An increasing value of N_{Lo} makes the surface interaction more attractive while a much decreasing value of N_{Lo} makes the net surface interaction repulsive for certain values of separation. When the EDL force is negligible, the effect of N_{E1} and N_{DL} on the efficiency is also insignificant, but the effect of N_{Lo} and N_{Rtd} on the efficiency is considerable because the efficiency is an increasing function of N_{Lo} and a decreasing function of N_{Rtd} (19, 20). Consequently, the results in Fig. 2 indicate that the value of the efficiency undergoes a step function change to virtually zero at certain threshold values of N_X corresponding to the presence of a net repulsion interaction force between the particle and collector while on either side of the threshold value the value of the efficiency remains constant (18).

To date, studies have almost exclusively examined ionic strength effects, and there have been few fundamental studies which have addressed or quantified the effect of the surface chemistry of the interacting surface with respect to the solution chemistries explored. This suggests a need for additional experimental investigation to study particle transport in porous media under carefully controlled chemical conditions and to account for and quantify both the ionic strength and specific chemical interaction aspects of chemical effects on EDL repulsive forces. There is also a need for a critical review of the possible reasons for the failure of the Derjaguin-Landau-Verwey-Overbeek (DLVO) theory including a quantification of the magnitude of the effects where possible.

MATERIALS AND METHODS

Suspended Particles

Three different sizes of latex particles were utilized in the present study. All of the particles were monodispersed microspheres coated with yellow-green fluorescent dyes. These fluorescent monodispersed microspheres contain carboxylate surface functional groups. The other properties of the particles as provided by the supplier and/or manufacturer are that mean diameters are 0.093 (std. dev. = 0.001), 1.16 (0.012), and 9.33 (0.64) μm; monomers are styrene; weight of polymer is 0.025 g/cm^3 in latex; density of polymer is 1.05 g/cm^3; refractive index (at 540 nm) is 1.59; surface charge is negative; pH at the point of zero proton condition (pH_{PZPC}) ranges from 2.5 to 3.0; and potential determining ions are H^+ and OH^-.

All of the particles were shipped in deionized water, stored at 4°C, and protected from light or freezing. The particles were provided by Polysciences, Inc., Warrington, Pennsylvania. In this work latex particles of 0.093, 1.16, and 9.33 μm are referred to as the nominal 0.1, 1.0, and 10 μm particles, respectively.

Deionized and glass distilled water (DI water), produced by using a Corning Megapure distillation system, was employed for all experimental works. Concentrated colloid solutions (original) were diluted to the stock solutions using unaltered DI water. The stock colloid solutions were stored at 4°C and diluted to the working solutions as needed, using DI water. The pH of DI water was typically near 5.6.

Particle size distribution (PSD) measurements were made using a flow cytometer manufactured by Epics Elite and a transmission electron microscope (TEM). The results of PSD measurements of 0.1, 1.0, and 10 μm particles indicated number-average mean diameters of 0.091, 1.2, and 9.1 μm with coefficients of variation of 7.8, 3.1, and 9.7%, respectively. Secondary electron images (SEI) of the 0.1- and 1.0-μm particles were made with a Philips Model 301 Transmission Electron Microscope (TEM), while SEI of the 10-μm particles was made with a Jeol Model 840 Scanning Electron Microscope (SEM). The SEIs produced with SEM and TEM illustrated a greater degree of polydispersity of size for the 10-μm particles as compared to the 0.1- and 1.0-μm particles. The SEI of the 10-μm particles at 7000 times magnification showed the sphericity and smoothness of the latex particles (21). The zeta potential of latex particles in electrolyte solutions was measured by a Model 501 Laser Zee Meter manufactured by Pen Ken, Inc., employing the technique of microelectrophoresis.

Porous Media

The porous media utilized for the colloidal particle transport experiments were comprised of columns of glass beads. The glass beads had properties of soda-lime glass and were provided by Polysciences, Inc., Warrington, Pennsylvania. The properties of the beads are that the surface functional group in water is an amphoteric surface silanol group (>SiOH), surface charge is negative, pH_{PZPC} is 2.5–3.0, and potential determining ions are H^+ and OH^-. The beads are specified as being 90% true spheres with less than 5% irregular shaped particles. Three sizes of glass beads were employed for this study. The average diameters of the spheres were approximately 0.13 (0.1–0.15), 0.28 (0.25–0.3) and 0.63 (0.5–0.75) mm. In this work the packed columns using glass beads sizes of 0.63, 0.28 and 0.13 mm are referred to as Column I, Column II, and Column III, respectively.

The SEI of the 0.28-mm glass beads at 40 times (which were made using the Jeol Model 840 SEM) showed the general sphericity of the beads while the image at 7000 times magnification showed generalized small-scale surface roughness features. The roughness appeared to be approximately ~0.5 to 4 μm in width. The large pits (~1 to 2 μm deep) were found to occur randomly over the glass surface (21).

The streaming potential of glass beads was measured by using the apparatus (porous plug) designed by the authors (21). The streaming potential was measured for only the 0.28-mm-sized glass beads (Column II) because all three sizes of glass beads had the same properties of soda-lime glass. The zeta potential of glass beads was calculated with data of the streaming potential measurement, using the Helmholtz–Smoluchowski equation (21).

The glass beads were cleaned prior to packing in the columns for the transport experiments. The beads were cleaned by soaking in an ultrasonic bath with DI water, 0.02 M NaOH, DI water, 1.0 M H_2SO_4, and DI water, successively. After the final rinse, the beads were dried overnight in an oven at 70 to 80°C and then stored in an acid-washed Pyrex beaker. The glass beads and columns were cleaned and repacked frequently to prevent debris from building up in the columns.

Packed Columns

The transport apparatus consisted of the following major components: Solution Reservoirs, Peristaltic Pumps, Tubing and Connectors, Constant Head Tanks, Head Adjustors, Dust Covers, and Packed Columns. A schematic of the transport apparatus is presented in Fig. 3. The transport apparatus was composed of two groups of columns fed by either a sodium chloride solution or a calcium chloride solution. They were controlled by clamps. One electrolyte solution flowed through one group of columns (three columns). Packed columns were fabricated from cast acrylic tubing with a nominal inside diameter of 1.0 cm and a length of 111 cm. The bottom of the column (inlet) was supported with a cotton plug. The required amount of glass beads to yield a specific bed depth in the columns was determined by measuring the volume in the empty column to the required depth. The bead volume was calculated using a porosity of 0.37, and the required weight of dried beads was determined by using a glass density of 2.48 g/cm^3. The calculated amount of cleaned and dried glass beads was packed to the predetermined level of the column. After packing, the columns were conditioned for 3 days by flowing DI water through them. When stabilized, the hydraulic conductivities of the columns were

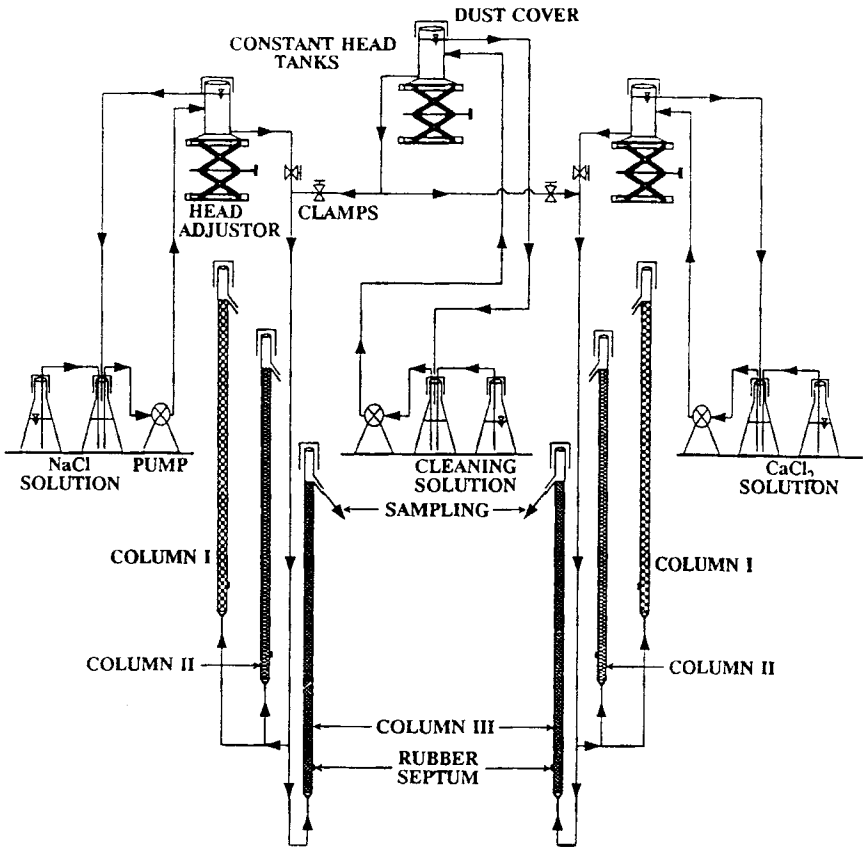

FIG. 3 Schematic diagram of the colloidal particle transport apparatus.

0.124, 0.031, and 0.006 cm/s for Columns I, II, and III, respectively. The constant head tanks and the columns were fabricated at an on-campus machine shop according to the authors' design. The entire apparatus was periodically cleaned and disinfected using Clorox bleach.

Particle Transport Experiments

The colloidal particle transport experiments involved measuring the concentration of latex particles that entered and passed through a column of glass beads as a function of time under different chemical conditions and different flow rates. The packed columns were cleaned, packed, and stabilized before starting all transport experiments. The first step in per-

forming a transport experiment was to set the desired flow rate. The desired flow rate was set by adjusting the head difference between the water level of the constant head tank and the outlet of the column. The solution flowed upward from the bottom of the column. The actual flow rates varied approximately ±3% from the nominal flow rates of 70 mL/day (0.9 m/day superficial velocity) and 210 mL/day (2.7 m/day superficial velocity).

The electrolyte solutions were made with NaCl or $CaCl_2$, and their pH was adjusted with 0.1 M NaOH or H_2SO_4. The actual electrolyte concentrations to be used in this work were 10^{-2} and 10^{-3} M NaCl, 5×10^{-4} and 5×10^{-5} M $CaCl_2$, and combinations of both electrolytes. The actual pH values of the electrolyte solution were near 3.0, 5.1, and 9.1. The pH of the influent was monitored at the head tank several times during stabilizing of the columns with the actual electrolyte solution. If needed, the pH in the head tank was adjusted. The pH of the effluent was measured for the first transport run sample. If the pH value of the influent was about 9.1, the pH value of the effluent was equally about 9.5 for the three columns used. However, if the influent pH was about 5.1, the effluent pH values were approximately 6.7, 9.5, and 9.5 for Columns I, II, and III, respectively.

The colloidal particle samples for injection were prepared by diluting the stock colloid solution with the same electrolyte solution as that used for the flow. The particle concentration of injection solution was determined with the concentration to minimize particle–particle collisions in a packed column as well as to detect the particle in the effluent. The samples were prepared a day before injecting and stored at 4°C. The samples were taken out of the refrigerator about 4 hours prior to injection to be warmed up to room temperature. The particle concentrations for injection are shown in Table 2. The 1-mL particle sample was injected by using

TABLE 2
Particle Concentrations for Injection

Property	Value		
	0.1 μm Particle	1.0 μm Particle	10 μm Particle
Particle number of original (no./mL)	4.55×10^{13}	4.55×10^{10}	4.55×10^{7}
Particle number of stock solution (no./mL)	4.55×10^{10}	4.55×10^{7}	4.55×10^{5}
Particle number of injection solution (no./mL)	9.10×10^{8}	4.55×10^{5}	4.55×10^{3}

a 1-mL hypodermic syringe. The sample was slowly injected into the column, and approximately 45 seconds were taken per injection.

The effluent samples of the transport run were taken by using 10 and 100 mL graduated cylinders. The effluent samples were taken at predetermined times based on the results of tracer experiments (21). The first sample was taken after 8 hours elapsed for the 0.9 m/day system and 2 hours elapsed for the 2.7 m/day system. After taking the first sample, the remaining samples were taken every 1.5 or 2 hours for the 0.9 m/day and every 30 minutes for the 2.7 m/day. Effluent samples were collected during an 18-hour period for a superficial velocity of 0.9 m/day and during a 6-hour period for a superficial velocity of 2.7 m/day. The effluent particle concentrations were determined by measuring the fluorescence of the particles using a Model 112 Turner Digital Filter Fluorometer. Standard measurements were always conducted right after the sample measurements using several concentrations of the standard particle solution constituted of one particle size, which were prepared from the same stock colloid solutions as those used for the preparation of injection particle solutions.

After a transport run experiment was completed, the flow of the electrolyte solutions was stopped and replaced with a cleaning solution (pH 9.5–10, no electrolyte). The cleaning solution flowed through both groups of columns at the rate of 10–25 m/day for 12 hours to wash out the retained particles in the columns. After finishing the cleaning procedure, the columns were flushed using electrolyte solutions at the same rates as those used during the cleaning process.

Tracer Transport Experiments

In order to characterize a flow of solution through the packed column, experiments were made using a conservative tracer. The procedure used for a tracer experiment was essentially the same as for a colloidal particle transport experiment. A 1000-mg/L NaBr stock solution was used in place of the latex particles. The concentrations of Br^- in standard solutions and effluent samples were measured by using an Orion Model 94-35 bromide electrode connected to an Orion Model 701A digital Ionalyzer. The samples were collected every hour for the 0.9 m/day and every 15 minutes for the 2.7 m/day.

The results of the tracer experiments were used to observe the combined effects of the injection section, porous media, and exit section of the packed column on the dispersion of the pulse input of tracer. The results were used to establish appropriate sampling times for the particle transport experiments. The mean hydraulic residence times (t_{mean}) calculated from

the results of the tracer experiments were 10.34 hours for the 0.9 m/day system and 3.39 hours for the 2.7 m/day system.

RESULTS AND DISCUSSION

The overall results of the particle transport are presented in Table 3. The results of the colloidal particle transport experiments and the zeta potential measurements are presented together for each type of latex particle. All values of particle throughput are averages for several experiments in the same column and chemical condition.

Brownian Particle Transport

Chemical effects on the transport of the 0.1-μm particles were investigated by varying solution pH. The results observed at pH values of 5.1 and 9.1 at 10^{-3} M NaCl and 5×10^{-4} M $CaCl_2$ are presented in Table 3. At 10^{-3} M NaCl the changes in ζ-potential corresponding with a pH change from 9.1 to 5.1 are 24.4 and 34.3% for the particle and collector, respectively. For a superficial velocity of 0.9 m/day, the corresponding decreases in transport rate (for the changes of ζ-potential) are 85.1, 70.6, and 45.9% for Columns I, II, and III, respectively.

In Table 3, comparing the ζ-potentials at 5×10^{-4} M $CaCl_2$ and a pH of 9.1 with the ζ-potentials at 10^{-3} M NaCl and a pH of 9.1, the former is 65.8 and 60.8% less than the latter for the 0.1-μm particles and collector, respectively. For the velocity of 0.9 m/day, the corresponding decreases in particle throughput are 64.4, 67.7, and 56.4% for Columns I, II, and III, respectively. Comparing the ζ-potentials at 10^{-3} M NaCl and a pH of 9.1 with the ζ-potentials at 5×10^{-4} M $CaCl_2$ and a pH of 9.1 and the ζ-potentials at 10^{-3} M NaCl and a pH of 5.1, the former is decreased about two times more than the latter. However, the decreases in the particle throughput corresponding with a decrease in the ζ-potential are larger at 10^{-3} M NaCl and a pH of 5.1 than at 5×10^{-4} M $CaCl_2$ and a pH of 9.1. Therefore, these results indicate that a change in pH has a greater effect on particle transport in the packed column than a change in charge concentration. In this study, at 5×10^{-4} M $CaCl_2$ and a pH of 9.1, the particle throughput suddenly decreased with decreasing pH below 8.0; at 10^{-3} M NaCl and 5×10^{-5} M $CaCl_2$ at a pH of 5.1, the particle throughput abruptly decreased with decreasing pH below 4.8 (18, 21). Even though only a small amount of pH variation existed, it usually caused a large change in the particle throughput. It appears that variation of pH is the

TABLE 3
Summary of Particle Transport Experiments[a]

Chemical conditions (M)			Particle size	Fraction transported (%)[b]						Zeta potential,[c] (mV)	
				0.9 m/day			2.7 m/day				
$[Na^+]$	$[Ca^{2+}]$	pH	(μm)	I	II	III	I[d]	II[d]	III[d]	$-\zeta_p$[e]	$-\zeta_c$[e]
10^{-3}	—	9.1	0.1	87.3	80.6	90.5	39.0	36.4	34.0	80.0	63.3
			1.0	100.2	90.2	72.8	94.9	90.8	67.8	81.3	63.3
			10.0	10.3	11.1	11.9	16.1	18.6	21.9	45.5	63.3
10^{-2}	—	9.1	0.1	76.5	54.0	70.9	23.3	36.4	32.5	86.2	38.4
			1.0	82.9	53.1	38.7	67.4	69.9	44.3	77.7	38.4
			10.0	0.0	0.0	0.0	—	—	—	55.6	38.4
—	5×10^{-5}	9.1	0.1	35.4	33.4	33.5	41.2	51.1	48.3	43.4	53.2
			1.0	96.0	86.0	50.7	87.8	68.6	62.2	54.6	53.2
			10.0	0.0	0.0	0.0	16.6	25.1	16.2	49.5	53.2
—	5×10^{-4}	9.1	0.1	22.9	12.8	34.1	26.9	28.7	58.7	27.4	24.8
			1.0	52.2	29.8	24.4	77.0	44.4	41.2	35.7	24.8
			10.0	0.0	0.0	0.0	—	—	—	30.1	24.8
—	10^{-3}	9.1	0.1	—	—	—	—	—	—	—	15.9
			1.0	12.7	0.2	2.1	—	—	—	—	15.9
			10.0	—	—	—	—	—	—	—	15.9
10^{-3}	—	5.1	0.1	2.2	10.0	44.6	9.0	29.3	30.1	60.5	41.6
			1.0	57.8	47.0	31.0	47.3	64.2	72.6	63.2	41.6
			10.0	0.0	0.0	0.0	—	—	—	44.1	41.6
10^{-3}	—	3.0	0.1	—	—	—	—	—	—	17.3	12.0
			1.0	0.0	0.0	0.0	—	—	—	0.4	12.0
			10.0	—	—	—	—	—	—	0.0	12.0
—	5×10^{-5}	5.1	0.1	0.8	0.6	53.2	17.3	24.8	43.3	34.9	51.8
			1.0	56.5	44.6	32.9	73.0	73.2	57.3	38.0	51.8
			10.0	—	—	—	—	—	—	32.9	51.8
10^{-3}	5×10^{-5}	9.1	0.1	31.2	17.7	28.7	—	—	—	57.3	44.9
			1.0	92.5	77.5	28.7	95.0	50.2	71.6	71.5	44.9
			10.0	0.0	0.0	0.0	—	—	—	57.4	44.9
10^{-3}	5×10^{-4}	9.1	0.1	0.0	0.0	1.3	—	—	—	43.3	27.5
			1.0	0.0	0.0	0.0	48.2	15.3	20.1	42.0	27.5
			10.0	—	—	—	—	—	—	29.4	27.5

[a] A dash "—" means there was no experiment.

[b] All data are averages of several measurements in the same column and chemical conditions.

[c] All data are averages of several measurements.

[d] Collector sizes are Column I (0.5–0.75 mm), Column II (0.25–0.3 mm), and Column III (0.105–0.15 mm).

[e] The zeta potentials of the particle and collector (ζ_p and ζ_c) for a pH of 9.1 were actually measured at a pH of 9.5. All measured values are averages of several experiments for the particle and collector in the same chemical conditions.

most important factor for consistent results. The possible reasons for the phenomena mentioned above is explained below.

There is a surface regulation interaction between the ionizable surfaces approaching one another, which is generally a feedback mechanism that is able to work due to the buffer capacity of the surface. In this case the measured repulsive force usually lies between calculated values for constant surface charge (CSC) and constant surface potential (CSP) during the regulation interaction (22). In this work, H^+ and OH^- are potential determining ions (PDIs) for both the particle and collector utilized, and have the effect of regulating both surface potential and charge directly. Calcium ions may regulate the potential and charge through coordination with the surface functional groups, where the existence of a Stern layer is significant. In this work, pH_{PZPC}s for both the particle and the collector occur below about 3.0. Under the conditions of 10^{-3} M NaCl and a pH of 5.1, positive, neutral, and negative sites ($>SiOH_2^+$, $>SiOH$ and $>SiO^-$) may exist simultaneously. As the two surfaces are brought together, dissociation of the positive sites occurs to maintain equilibrium causing the surface charge to decrease. This results in a decrease in the surface potential (23). In this case the reaction may create a CSP condition, and regulation will occur because the surface potential is controlled by only the PDIs (H^+ and OH^-). Under potential regulating conditions, changes in surface potential are minimized at the expense of surface charge, that is, the surface charge must be zero at zero separation. Surfaces that can regulate charges will in general coagulate at lower salt concentrations and will form more ordered structures at higher volume fractions than will surfaces that cannot regulate charges. Ruckenstein and Prieve (13) have indicated that small changes in the surface potential lead to very large changes in the "activation energy," and consequently, great changes in the deposition rate. They also stated that a 5 mV decrease in the surface potential can increase the deposition rate by six orders of magnitude.

However, at 5×10^{-4} M $CaCl_2$ and a pH of 9.1, the surfaces may be almost fully dissociated. Here the surface charge is an insensitive function of the surface potential, and regulation will be poor. Furthermore, the Stern layer adjustment time (the average time needed for displacement of ions across the Stern layer) is much longer than the time of a Brownian encounter of the two surfaces (the average time needed for a particle to travel through the thickness of the double layer). Thus, the system cannot be regulated during the time of Brownian collision. In this case the system approaches a CSC condition (23). At the CSC condition the surface potential must increase as the surfaces approach each other (24).

The effects of 5×10^{-5} and 5×10^{-4} M $CaCl_2$ solutions at pH of 9.1 on the transport of the 0.1-μm particles are presented in Table 3. The results show that particle throughput levels are decreased systematically as the calcium concentration is increased. Particle transport decreases with increasing calcium concentration due to specific interaction of Ca^{2+} with the particle and collector surfaces like a PDI (25). When Ca^{2+} is adsorbed on the particle and collector with surface functional groups and surface potentials are constant, the EDL is compressed and PDI adsorption reactions are then facilitated and more PDI are forced to adsorb at the surface in order to maintain a constant surface potential. This interaction results in decreasing particle and collector ζ-potentials and a reduced EDL repulsive force. The decreased transport may be the results of the reduced repulsive energy barrier.

At a superficial velocity of 0.9 m/day and a pH of 9.1, comparing the particle throughput for 10^{-2} M NaCl with that for 5×10^{-5} M $CaCl_2$, the particle throughput of the former (67%) is approximately double that of the latter (34%) even though the EDL thickness ($1/\kappa$) of the 10^{-2} M NaCl is about 3 nm while that of the 5×10^{-5} M $CaCl_2$ is about 25 nm (26, 27). The results indicate that the effect of divalency is predominant to that of ionic strength (sodium ion) on the decreasing particle transport. In this work the sodium ion is an indifferent ion (IDI).

As shown in Table 3, the effects of combined electrolytes on the transport of 0.1-μm sized particles are quite significant. The combined use of 10^{-3} M NaCl is shown to reduce the particle throughput levels for 5×10^{-5} and 5×10^{-4} M $CaCl_2$ at a pH of 9.1. One possible reason for this may be that 10^{-3} M NaCl caused a greater compression of the EDL thickness and so the SIFBL becomes thin and the contact between the particle and collector surfaces may be easily achieved. Consequently, one conclusion which is taken from the chemical effects discussed previously is that pH exerts the most effect on the transport/deposition of the particle in the packed column. The next greatest effect on the particle transport appears to be the combined electrolyte, calcium ion, and sodium ion in that order.

The changes in particle throughput that result from the changing chemical conditions parallel the expected variations in the repulsive EDL interaction force that arises between the particle and collector at close approach. The decrease in throughput occurs as the magnitude of the negative ζ-potential of the particle and collector surfaces (which have negative surface charge) is decreased by increasing the electrolyte concentration, ionic valency, and/or decreasing pH. The increase in ionic strength and/or ionic valency causes the thickness of the diffuse layer ($1/\kappa$) to decrease. For example, comparing solutions of a 1 : 1 electrolyte with those

of a 3:3 electrolyte, it follows from the definition of κ that the same value of κ can be calculated from one-ninth molar concentration of the trivalent or a molar concentration of the monovalent (26, 28). This allows the particle to come closer to the collector surface before a repulsive EDL force will arise. Thus, as the separation distance decreases, the LVDW attractive force increases dramatically such that a net repulsive surface interaction force barrier can be eliminated. For this situation, increases in the flow velocity may cause a small change in particle throughput.

Throughputs of 0.1 μm particles observed at a chemical condition of 10^{-3} M NaCl and pH of 9.1 and superficial velocities of 0.9 and 2.7 m/day are shown as cumulative F curves in Fig. 4. In the figure the fractions of the influent particle concentration reaching the effluent, C/C_0, were calculated from C curves of the pulse input, and are plotted as a function of dimensionless time, t/t_{mean}, where t_{mean} is the mean hydraulic residence time determined from tracer experiments. t_{mean} was 10.34 and 3.39 hours, respectively, for superficial velocities of 0.9 and 2.7 m/day

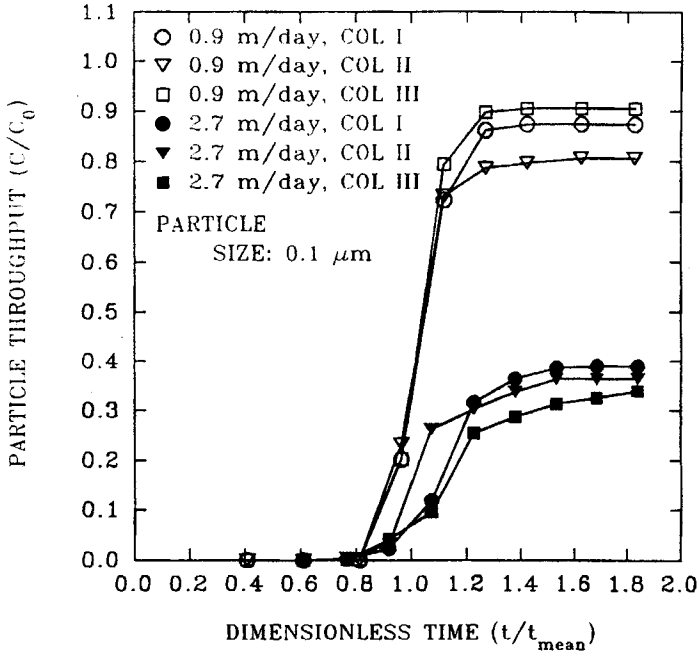

FIG. 4 Cumulative F curves. Fraction of the influent particle concentration transported through the column as a function of dimensionless time (0.1 μm particles, 10^{-3} M NaCl, pH ≈ 9.1, $U \approx 0.9$ and 2.7 m/day).

(flow rates of 70 and 210 mL/day). Large amounts of particle throughput were observed for a superficial velocity of 0.9 m/day. However, when the superficial velocity was increased to 2.7 m/day, particle throughput suddenly decreased from 87.3% at 0.9 m/day to 39% at 2.7 m/day even though particle and collector ζ-potentials (ζ_p and ζ_c) were -80 and -63.3 mV, respectively (Column I). This suggests a high repulsive energy barrier. Additional experiments were made using Brownian particles of 0.1 and 1.0 μm at the same solution chemistry, the same column (Column I), and two different flow rates of 1400 and 7000 mL/day (superficial velocities of 18.3 and 89.8 m/day). The results of these experiments are presented in Fig. 5. As shown in this figure, the 0.1-μm particle throughput was almost unchanged from that (about 40%) observed at a superficial velocity of 2.7 m/day even though the superficial velocity had been increased to 18.3 m/day. The particle throughput increased to 81% when the superficial velocity was increased to 89.8 m/day. In all cases the throughput of 1.0

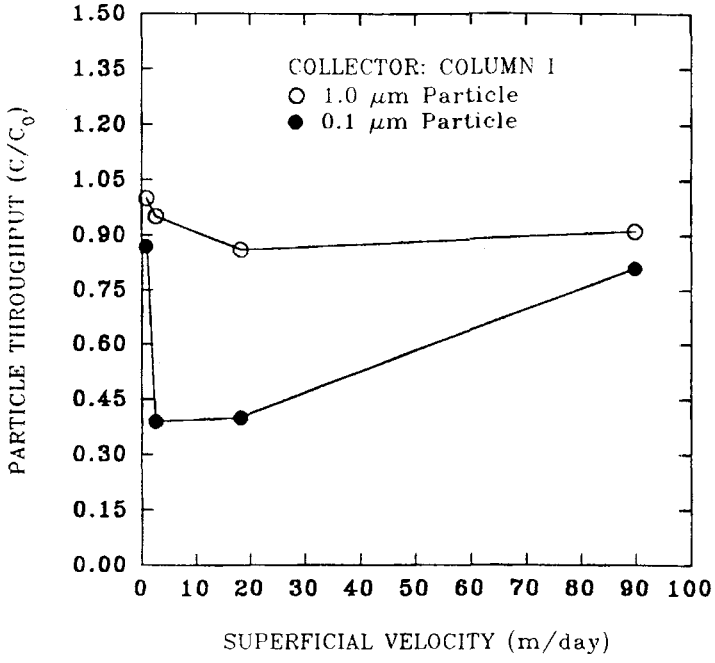

FIG. 5 Variations in particle throughput with increasing superficial velocity (0.1 and 1.0 μm particles, 10^{-3} M NaCl, pH ≈ 9.1, U ≈ 0.9, 2.7, 18.3, and 89.8 m/day).

μm particles revealed the same trend as that of 0.1 μm particles, but the throughput was much greater. In Table 3 the same trend for the 0.1- and 1.0-μm particles is also shown for 10^{-2} M NaCl and pH of 9.1, whereas the opposite trend is shown for 5×10^{-4} M $CaCl_2$ and pH of 9.1, and for 5×10^{-5} M $CaCl_2$ and pH of 5.1.

Consequently, it appears that at a superficial velocity of 0.9 m/day, particle transport was mainly controlled by surface interaction forces, that is, hydrodynamic action was not important. Several possible explanations for this are given in the following paragraphs.

When two rough surfaces approach each other very closely, surface roughness causes the LVDW attraction to be reduced as compared to the interaction of smooth surfaces. The ratio of the attraction for rough surfaces to the attraction for smooth surfaces is proportional to the ratio of the separation distance between the outermost points on the surfaces to the separation distance between the mean profiles of the surfaces (29–31). On the other hand, a lesser extent of EDL overlap is expected for rough surfaces as compared to smooth surfaces for a given separation distance (31). An important issue is the comparison between the reduction in the EDL interaction force and the reduction in the LVDW force. If the relative reduction in the EDL interaction is greater for rough surfaces than for smooth surfaces, net attraction might result for rough surfaces. For a case where net repulsion for smooth surfaces is predicted, significant local net attractive energy minima are predicted to occur for rough surfaces. The local energy minima give rise to tangential forces that can oppose hydrodynamic drag forces and lead to particle capture at these locations.

The variation in interaction energy is caused by surface roughness, heterogeneous surface site distributions, and discrete surface sites. The DLVO theory assumes that the height of the energy barrier remains constant during particle–particle or particle–collector encounters. However, in every real system the barrier height, and thus the interaction energy, are subjected to perpetual random fluctuations due to reasons such as the random fluctuations in the concentrations of ions contained in the fluid between interacting surfaces and the translation and rotation of particles due to Brownian motions or fluid velocity gradients. Fluctuations of the interaction energy may increase appreciably the average flux of particles penetrating the energy barrier. Consequently, deposition or coagulation may occur in a system where no deposition is predicted using average or maximum values of the energy barrier if the fluctuation duration time (or the duration time of lower repulsive or of attractive energy) is longer than the diffusion relaxation time for crossing the energy barrier (the time required for a particle to travel across the barrier to a primary attractive region) (32).

A rigorous analysis of dynamic aspects of EDL interactions has only recently been undertaken. The results presented to date suggest that disequilibrium of the diffuse layer or of charge transfer (ion transport) in the Stern layers during the interaction of charged surfaces cause increased repulsive forces to arise as compared to the fully relaxed EDL interaction (33, 34). However, a rigorous coupling of hydrodynamic and electrochemical aspects of the dynamic interaction of particles with surfaces may alter this result. For example, the transport of ions caused by fluid escaping from the region between the approaching surfaces may interfere with the maintenance of an extensive diffuse layer and decrease the EDL repulsive force. If the LVDW force was significant at this separation distance, the net force might be attractive in a system for which the classical DLVO leads to a prediction of net repulsion.

For Brownian particles like 0.1 μm, the hydrodynamic retardation may be unimportant due to the characteristics of their size and Brownian movement. O'Melia (35) stated that hydrodynamic retardation reduces the deposition of large, almost neutrally buoyant alum flocs formed in conventional systems and is less important for the smaller, more dense particles applied to filters in direct filtration. In the present work, for 10^{-3} M NaCl and pH of 9.1 (high repulsive energy barrier and shallow secondary minimum), it appears that when the flow velocity increased from 0.9 to 2.7 m/day, decreases in the transport of 0.1 μm particles may have been caused by coupling hydrodynamic action with surface roughness. In reality, all surfaces are geometrically and energetically heterogeneous. Surface roughness and a nonuniform distribution of "active sites" are always present (13). The secondary electron image (the image of scanning electron microscope) showed that the collectors used in this work had certain irregularities. Some were protrusions and some were dentations (21). In the case where the separation distance between the surface of the particle and collector was less than 0.1 μm, some of the 0.1-μm particles may encounter the protrusions as the particles roll along the surface. At that point, for a case where net repulsion for smooth surfaces is predicted, significant local net attractive energy minima may be predicted to occur. This attractive force may be enough to overcome the repulsive energy barrier and then the particles may deposit on the surface. However, if the flow velocity increases (e.g., 89.8 m/day), this would probably cause a change in the flow pattern near the surface, which may result in a change in the Reynolds number, causing an instantaneous disturbance in the force balance at that point. The particle could swirl out of the collector surface, and decreases in the deposition may occur. Ives (12) has suggested that filtration efficiency is only attributed to a change in Reynolds number in the case where all the other transport mechanisms are either negligible or

held constant. Consequently, flow velocity or hydrodynamic action is an important factor in colloidal particle transport/deposition in porous media.

When the superficial velocity was increased from 0.9 to 2.7 m/day, the values of the particle throughput for 0.1 and 1.0 μm particles for each solution chemistry were averaged for Columns I, II, and III because the throughputs in Columns I, II, and IH followed the same trend with the exception of those in Column III for a pH of 5.1 and 0.1-μm particles (see Table 3). The results are presented in Figs. 6 and 7. In these figures the particle throughputs for 0.1 and 1.0 μm particles increased at all solution chemistries other than 10^{-3} and 10^{-2} M NaCl at pH of 9.1 and 10^{-3} M NaCl and 5×10^{-5} M $CaCl_2$ at pH of 9.1, respectively. The decrease at pH of 9.1 was much less intense for 1.0 μm particles than for 0.1 μm particles, while the increase at pH of 5.1 was much less intense for 0.1 μm particles than for 1.0 μm particles. At 5×10^{-4} M $CaCl_2$ and a pH of 9.1, the repulsive energy barrier may be negligible (21). At this condition the LVDW attractive force is greater than the repulsive EDL force over

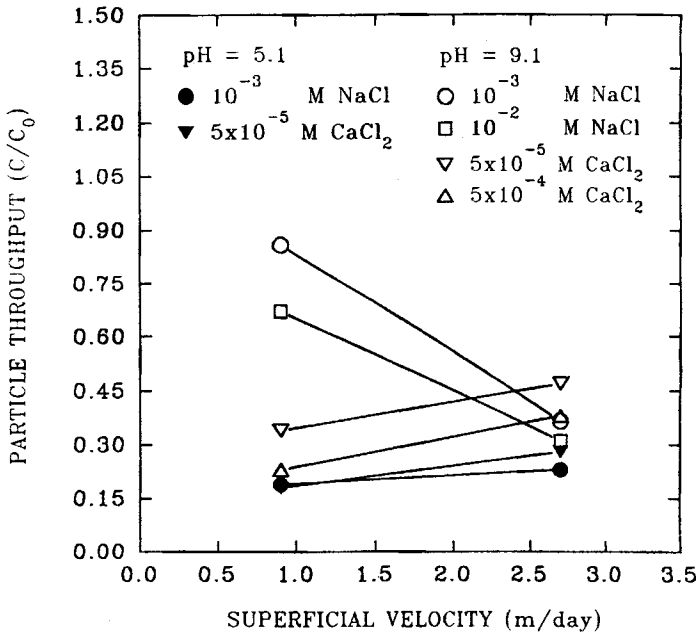

FIG. 6 Variations in particle throughput with increasing superficial velocity (0.1 μm particles, pH ≈ 5.1, and 9.1, $U \approx 0.9$ and 2.7 m/day; each curve is for a different concentration of NaCl and $CaCl_2$).

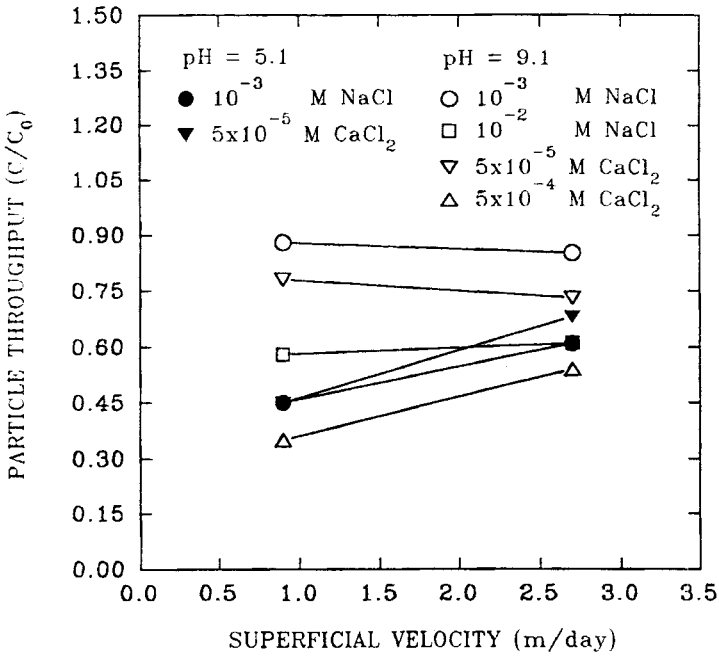

FIG. 7 Variations in particle throughput with increasing superficial velocity (1.0 μm particles, pH ≈ 5.1, and 9.1, $U \approx 0.9$ and 2.7 m/day; each curve is for a different concentration of NaCl and $CaCl_2$).

almost all separation distances, and the rapid deposition may be accomplished according to DLVO theory. Thus, increases in the flow velocity may cause a small change in particle throughput (36).

Rajagopalan and Kim (36) conducted an experiment on the deposition of Brownian particles on a rotating disk under several chemical conditions and fluid velocities (very small Peclet number and very large Peclet number). They found that the magnitude of the deposition rate is strongly influenced by three interconnected factors: the depth of the secondary minimum, the repulsive energy barrier, and the flow velocity (listed roughly in the order of their importance). For instance, in the case of high repulsive energy barrier and shallow secondary minimum, increases in the Peclet number (i.e., increases in the flow velocity) lead to increases in the particle deposition, and these increases are small. However, in the intermediate case in which the maximum repulsive barrier is close to zero

and the deep secondary minimum is large in magnitude, increases in the Peclet number lead first to an increase in the deposition and subsequently to decreases in the deposition because of the changing importance of normal convection over radial convection. The decrease in the deposition results from the increasing radial convection of the particles and the large values of the particle concentration in the secondary minimum. They also reported that the deposition rate is generally directly proportional to the concentration near the secondary minimum. The deposition by the secondary minimum is considered reversible (adsorption and desorption) (37). In this work the deposition experiments were made in porous media. Both increases in the flow velocity in the porous media and increases in rotational speed of a disk are considered to have the same effects for the particle deposition because the rotational velocity is used to calculate the Peclet number of the rotating disk like a superficial velocity is used to calculate the Peclet number of the packed column. In the present study it may be considered that the energy profiles at 10^{-3} M NaCl and 5×10^{-4} M $CaCl_2$ and pH 9.1 are consistent with those at the high repulsive barrier with shallow secondary minimum and the intermediate case of Rajagopalan and Kim (36), respectively. Therefore, it appears that the deposition process of Brownian particles for physicochemical conditions of this work is consistent with that of Rajagopalan and Kim (36).

The transport experiments for 1.0 μm particles were made using the same physical and chemical conditions as those used for 0.1 μm particles. The results are presented in Table 3. Particle throughputs observed at chemical condition of 10^{-3} M NaCl and pH of 9.1 and superficial velocities of 0.9 and 2.7 m/day are shown as cumulative F curves in Fig. 8. With a change in the solution chemistry, the transport of 1.0 μm particles changed systematically as did that of 0.1 μm particles. However, there is a somewhat different trend in throughput between 0.1 and 1.0 μm particles, depending upon the collector size and the flow velocity. In Table 3, as far as the collector size is concerned, at a superficial velocity of 0.9 m/day and all solution chemistries used, 1.0 μm particle throughput was greatest in Column I (the largest of the three different collector sizes used) and smallest in Column III (the smallest collector size used). On the other hand, 0.1 μm particles produced throughput results opposite to those for 1.0 μm particles. Particle throughputs at a superficial velocity of 2.7 m/day showed, as for the collector size, similar trends to those at 0.9 m/day. As for the change of physicochemical conditions, some exceptional results were produced for both 0.1 μm particles and the smallest collector size. The origin of the above phenomena has not been fully investigated, but some tentative deductions can be made from the experimental data and the literature reviewed.

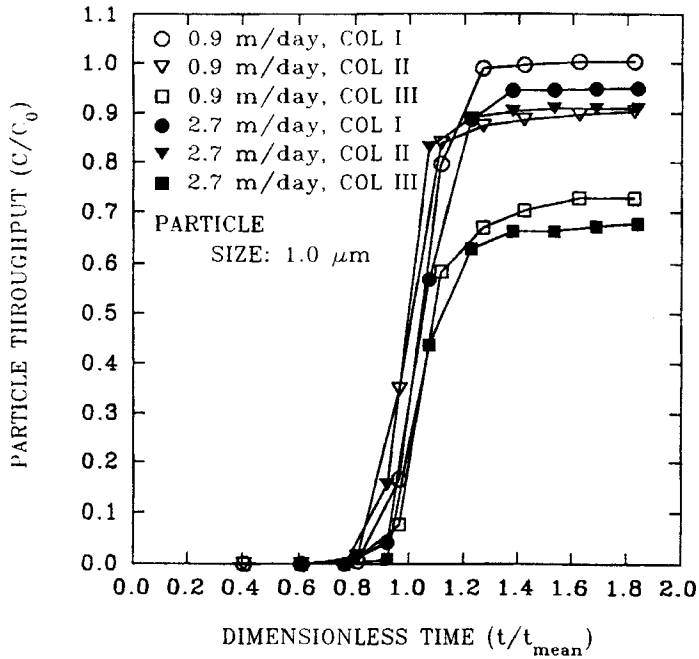

FIG. 8 Cumulative F curves. Fraction of the influent particle concentration transported through the column as a function of dimensionless time (1.0 μm particles, 10^{-3} M NaCl, pH ≈ 9.1, $U \approx 0.9$ and 2.7 m/day).

The latex particles used in this work have the same surface chemical properties, and only differ in size. As shown in Table 3, the zeta potentials of 0.1 and 1.0 μm particles were approximately the same at all solution chemistries used (i.e., the difference is 4.8 mV in average). Therefore, it may be considered that all of the above phenomena, which show opposite throughput responses for 0.1 and 1.0 μm particles depending on the collector size, were caused by the difference in their Brownian diffusivity. For water at 22°C the Brownian diffusivities for 0.1 and 1.0 μm particles are 4.51×10^{-8} and 4.51×10^{-9} cm^2/s respectively, which are small but significant within pore spaces. For particles greater than about 1.0 μm in diameter the viscous drag and inertia of the particle restrict the Brownian movement, and the mean free path (the mean magnitude of a random movement due to Brownian motion) of the particles is at most one or two particle diameters. The diffusive movement is not important in this case. For particles less than 1.0 μm the diffusive movement becomes increas-

ingly significant with decreasing sizes (12). Particle radius affects both the potential energy of interaction and the Brownian diffusion coefficient, and hence particle size influences the deposition rate under all conditions (38). The capture mechanisms for 1.0 μm particles balance between Brownian diffusivity and collection by interception and sedimentation (39). Under these conditions, 1.0 μm particles may be deposited only slightly in porous media. The effectiveness of removal by clean filter beds is a minimum for a suspended particle size of about 1.0 μm particles (32, 35). Submicron particles are deposited in porous media more efficiently due to their greater Brownian motion (12, 35). In this work the experimental data were consistent with this theory (see Table 3). Particle size (or particle size/collector size ratio) appears to be the most important factor for transport/deposition in the packed column. It may be considered that the combined effects of particle size, collector size, surface interaction force, and flow rate (flow velocity) in the packed column led to very complicated particle capture mechanisms (that indicate which combination gave the best removal and which gave the least removal) in the present study.

Non-Brownian Particle Transport

The transport experiments for 10 μm particles as a non-Brownian particle were made using the same solution chemistries, the same flow rates, and the same column conditions as those used for 0.1 and 1.0 μm particles. The results are presented in Table 3. Particle throughputs observed at chemical condition of 10^{-3} M NaCl and pH of 9.1 and superficial velocities of 0.9 and 2.7 m/day are shown as cumulative F curves in Fig. 9. With a change in the solution chemistry, the transport of 10 μm particles did not change systematically as did that of the 0.1- and 1.0-μm particles. When the flow velocity increased from 0.9 to 2.7 m/day, the increase in the particle throughput averaged out at 7.8 and 19.3% at 10^{-3} M NaCl and 5×10^{-5} M $CaCl_2$ and pH 9.1, respectively. This phenomenon is somewhat different from that of 0.1 and 1.0 μm particles. Hence, the results may indicate that the effect of solution chemistry was not significant in the transport of 10 μm particles in the packed column.

The capture mechanisms for particles larger than about 1.0 μm are interception and sedimentation (39). With increases in particle size, more particles can be removed by these mechanisms. Particles following fluid streamlines may collide with the collector by means of interception. This phenomenon is a function of interception parameter (a_p/a_c). Increases in the N_{RS} results in decreases in the separation distance between particle and collector. As shown in Fig. 2, particle removal by interception increases after passing through a minimum value. In this work, for 10 μm

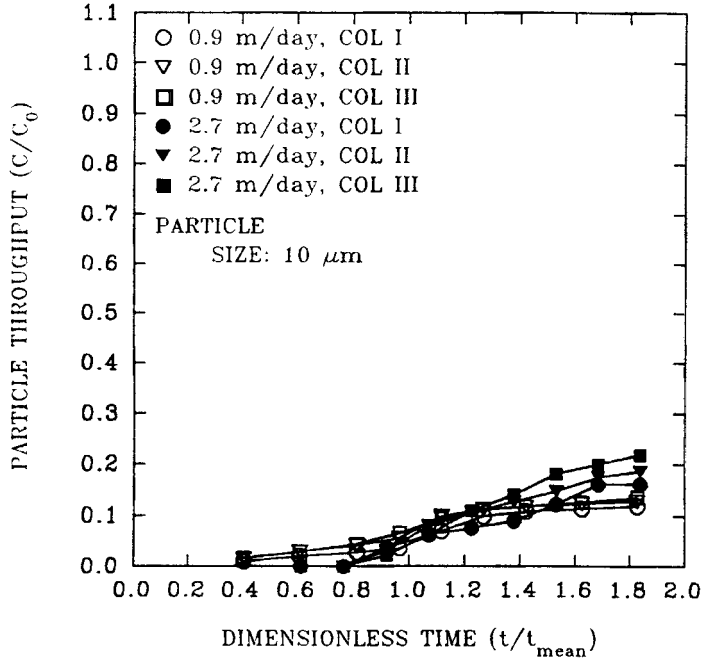

FIG. 9 Cumulative F curves. Fraction of the influent particle concentration transported through the column as a function of dimensionless time (10 μm particles, 10^{-3} M NaCl, pH $\approx$ 9.1, $U \approx$ 0.9 and 2.7 m/day).

particles, the magnitude of N_{RS} is approximately 0.01–0.025, 0.024–0.05 and 0.049–0.119 for Columns I, II, and III, respectively. All of the value are more than the minimum value of N_{RS} (see Fig. 2). Based on these data, it appears that there is a significant amount of deposition by interception in Column III. The results also indicate that the collection efficiency increased with increasing particle size and decreasing collector size when the capture mechanism was only by interception and when hydrodynamic retardation was neglected. In Fig. 2 an increase in drag resistance in the neighborhood of the collector is a function of the value of N_{RS}. That is, the hydrodynamic retardation increases as the value of N_{RS} increases. Hence, when the drag corrections are included in the trajectory analysis by Tien (18), the efficiency decreases with an increase in N_{RS} and a drastic decrease in the single collector efficiency is observed when $N_{RS} \geq 5 \times 10^{-3}$. In other words, hydrodynamic retardation causes a monotonic reduction in the collector efficiency to a minimum value as N_{RS} increases.

After passing the minimum value and if the N_{RS} continues to increase, inevitably the LVDW attractive force (the dimensionless group N_{Lo}) will dominate. As a result, the removal by interception increases. In the present study the magnitude of N_{Lo} was approximately 1.65×10^{-3} and 5.49×10^{-4} for a superficial velocity of 0.9 and 2.7 m/day, respectively (see Fig. 2). Consequently, in this work, interception was probably an important capture mechanism for 10 μm particles.

Considering only gravity forces, the single collector efficiency is shown as N_G in Table 1. In the present study the fluid flowed upward (the particles in the fluid flowed upward) so that the settling velocity was counterdirectional to the flow. Hence, N_G in Table 1 has a negative sign such as $-N_G$ (40). Rajagopalan and Tien (41) suggested that if the flow is upward, the force field near the collector becomes quite different from the case of the downflow. Fitzpatrick and Spielman (42) stated that experimental data and theory (developed under the conditions for settling codirectional to the flow) disagree significantly under conditions where the direction of gravity settling opposes the direction of flow. On the leading side of the collector, for the flow direction the gravitational force opposes collection and dominates the force due to fluid motion, since the fluid velocity (e.g., tangential velocity) diminishes as the separation distance decreases. On the trailing side of the collector, the gravitational force may promote particle collection (41). The negative contribution for the settling counterdirectional to the flow cannot exceed the positive contribution owing to interception, otherwise net collection is zero (40).

In this work the absolute value of N_G was about 0.3 and 0.1 for the superficial velocities of 0.9 and 2.7 m/day, respectively. The usual range of N_G in typical filtration systems lies above 10^{-4}, which is considered to be a very large N_G value. At 10^{-3} M NaCl and pH of 9.1, values of N_{E1} for 10 μm particles are 1.42×10^4 and 4.73×10^3 for the superficial velocity of 0.9 and 2.7 m/day, respectively, whereas a value of N_{E2} for 10 μm particles is 0.9. At 5×10^{-5} M $CaCl_2$ and pH of 9.1, values of N_{E1} for 10 μm particles are 4.36×10^3 and 1.45×10^3 for the superficial velocity of 0.9 and 2.7 m/day, respectively, whereas a value of N_{E2} for 10 μm particles is 1.0. These results indicate that there exist high repulsive energy barriers for these chemical conditions. In this study, even at the chemical conditions that produce high repulsive energy barriers, the fact that the deposition for 10 μm particles was achieved more than about 75% indicates that the deposition may have been accomplished by gravitational force and/or interception. Gravitational force was possibly more important under condition of low flow velocity (groundwater flow velocity). As shown in Table 3, increases in the flow velocity caused increases in the transport rate. This means that gravity settling was predominant.

CONCLUSIONS

The conclusions drawn from the results of this work are presented in the following paragraphs.

1. Chemical effects on particle transport in packed columns are the result of changes in surface interaction forces arising from specific interactions of ions and molecules with particle and collector surfaces and changes in ionic strength. Changes in the level of particle throughput are the result of changes in the chemical characteristics of the liquid phase when the physical characteristics of the solid phase are identical. For Brownian particles (0.1 and 1.0 μm), increases in ionic strength (through calcium ion addition) at pH of 9.1 decreases particle throughput, while decreases in solution pH at 10^{-3} M NaCl (as solution pH approaches pH_{PZPC}) decreases the particle throughput to an even lower level due to surface regulatory interaction. The effect of a low concentration of divalent ions (calcium ion) is superior to the effect of a high concentration of monovalent ions (sodium ion) in terms of decreasing particle throughput in packed columns. In this work it is speculated that calcium acts as a PDI through surface coordination reaction and sodium acts as an IDI. Sodium ions enhanced the effect of calcium ions on decreasing particle throughput. Consequently, one conclusion which can be taken from the chemical effects on Brownian particle transport in a packed column, is that pH is the most critical factor.

2. For non-Brownian particles (10 μm), changes in the solution chemistry do not cause systematic changes in particle throughput. Groundwater flow velocities are typically horizontal. Under such flow, sedimentation and interception are predominant capture mechanisms for non-Brownian particles, and thus capture can be made independent of ionic strength.

3. In the case of a high repulsive energy barrier and a negligible secondary minimum (e.g., 10^{-3} M NaCl and pH 9.1), increases in the flow velocity (0.9 to 89.8 m/day) cause large changes (first decrease and then increase) in particle throughput of 0.1 μm particles in Column I, whereas the transport of 1.0 μm particles shows a similar but less noticeable trend to that of 0.1 μm particles. Conversely, the transport rates of 10 μm particles increase when the flow velocity increases from 0.9 to 2.7 m/day. In the case of negligible repulsive energy barrier and deep secondary minimum (e.g., 5×10^{-4} M $CaCl_2$ and pH 9.1), an increase in the flow velocity (0.9 to 2.7 m/day) increases the transport rate of Brownian particles in all columns. Therefore, it may be considered that at the typical groundwater flow velocity (e.g., 0.9 m/day), Brownian particle transport is mainly governed by surface interaction forces, whereas non-Brownian particle transport is mainly governed by gravitational forces.

4. The reduced particle throughputs with increasing flow velocity at 10^{-3} M NaCl and pH of 9.1 were possibly caused by coupling both particle size and inhomogeneities of the surface of the particle and collector with hydrodynamic action. These inhomogeneities include surface roughness, heterogeneities in the distribution of charged surface groups, and the discrete nature of surface functional groups. Surface roughness causes the surface interaction forces to be reduced and the interaction energy to fluctuate as a particle travels along a collector surface. Fluctuations in interaction energy can also be caused by the rotation and translation of the particle relative to the collector when the surfaces are heterogeneous. The fluctuating energy or force barrier may allow deposition to occur at specific locations when the prediction based on average surface properties indicates no deposition. Hydrodynamic perturbations caused by surface roughness may also affect particle transport. The transport system used in this work was characterized by the interaction of smooth latex particles with relatively rough glass beads collector. The small-scale roughness of the glass beads was comparable to the distance over which EDL and LVDW interactions arise.

5. The difference of Brownian diffusivity between 0.1 and 1.0 μm particles caused the differences in the level of particle throughputs in Columns I, II, and III under the same chemical condition. The transport of 1.0 μm particles was the greatest in Column I and the smallest in Column III at all solution chemistries and superficial velocities of 0.9 and 2.7 m/day. The opposite response was noted for 0.1 μm particles. For the particle sizes studied, the 1.0-μm particles had the highest level of throughputs under all conditions.

6. Colloidal particle transport (deposition) in porous media is controlled by physical processes (i.e., Brownian diffusion, fluid motion, and gravity) and chemical processes (i.e., EDL repulsion and LVDW attraction). In this work the dominant capture mechanism for 0.1 μm particles was Brownian diffusion, whereas the dominant capture mechanisms for 10 μm particles were sedimentation and/or interception. For 1.0 μm particles, the particle–collector collisions were balanced between Brownian diffusion-dominated collisions and interception and sedimentation-dominated collisions.

ACKNOWLEDGMENT

This research was partially funded by the Water Resources Research Institute at Auburn University.

REFERENCES

1. J. F. Champlin, "The Physics of Fine-Particle Movement through Permeable Aquifers," *Soc. Pet. Eng. J.*, *12*, 367 (1971).
2. H. I. Nightingale and W. C. Bianchi, "Ground-Water Turbidity Resulting from Artificial Recharge," *Ground Water*, *15*, 146 (1977).
3. W. D. Robertson, J. F. LeBean, and S. Marcoux, "Contamination of an Unconfined Sand Aquifer by Waste Pulp Liquor: A Case Study," *Ibid.*, *22*, 191 (1984).
4. H. Bouwer, "Elements of Soil Science and Groundwater Hydrology," in *Groundwater Pollution Microbiology* (G. Bitton and C. P. Gerba, Eds.), Wiley-Interscience, New York, NY, 1984.
5. C. P. Gerba and G. Bitton, "Microbial Pollutants: Their Survival and Transport Pattern to Groundwater," in *Groundwater Pollution Microbiology* (G. Bitton and C. P. Gerba, Eds.), Wiley-Interscience, New York, NY, 1984.
6. B. H. Keswick and C. P. Gerba, "Virus in Groundwater," *Environ. Sci. Technol.*, *14*, 1290 (1980).
7. C. P. Gerba and S. M. Goyal, "Pathogen Removal from Wastewater During Groundwater Recharge," in *Artificial Recharge of Groundwater* (T. Asano, Ed.), Butterworths, Boston, MA, 1985.
8. L. M. McDowell-Boyer, R. H. James, and N. Sitar, "Particle Transport through Porous Media," *Water Resour. Res.*, *22*, 1901–1921 (1986).
9. M. Y. Corapcioglu and A. Haridas, "Transport and Fate of Microorganisms in Porous Media: A Theoretical Investigation," *J. Hydrol.*, *72*, 149–169 (1984).
10. M. Y. Corapcioglu and A. Haridas, "Microbial Transport in Soils and Groundwater: A Numerical Model," *Adv. Water Resour.*, *8*, 188–200 (1985).
11. K. M. Yao, "Influence of Suspended Particle Size on the Transport Aspect of Water Filtration," Unpublished Ph.D. Dissertation, University of North Carolina, Chapel Hill, NC, 1968.
12. K. J. Ives, "Capture Mechanisms in Filtration," in *The Scientific Basis of Filtration* (K. J. Ives, Ed.), Noordhoff International Publishing, Leyden, Netherlands, 1975.
13. E. Ruckenstein and D. C. Prieve, "Rate of Deposition of Brownian Particles under the Action of London and Double-layer Forces," *J. Chem. Soc., Faraday Trans. II*, *69*, 1522–1536 (1973).
14. D. C. Prieve and E. Ruckenstein, "Rates of Deposition of Brownian Particles Calculated by Lumping Interaction Forces into a Boundary Condition," *J. Colloid Interface Sci.*, *57*, 547–550 (1976).
15. T. E. Karis, "Diffusional Mass Transfer to a Rotating Disc," M.S. Thesis, Rensselaer Polytechnic Institute, Troy, NY, 1979.
16. R. Rajagopalan and C. Tien, "The Theory of Deep Bed Filtration," in *Progress in Filtration and Separation*, *1* (R. J. Wakeman, Ed.), Elsevier Scientific, New York, NY, 1979.
17. R. Rajagopalan and C. Tien, "Trajectory Analysis of Deep-Bed Filtration with the Sphere-in-Cell Porous Media Model," *Am. Inst. Chem. Eng. J.*, *22*, 523–533 (1976).
18. C. Tien, "Deep Bed Filtration," in *Handbook of Fluids in Motion* (N. P. Cheremisinoff and R. Gupta, Eds.), Ann Arbor Science, Ann Arbor, MI, 1983.
19. A. C. Payatakes, C. Tien, and R. M. Turian, "Trajectory Calculation of Particle Deposition in Deep Bed Filtration: Part II. Case Study of the Effect of the Dimensionless Groups and Comparison with Experimental Data," *Am. Inst. Chem. Eng. J.*, *20*, 900–905 (1974).
20. R. Rajagopalan and C. Tien, "Single Collector Analysis of Collection Mechanisms in Water Filtration," *Can. J. Chem. Eng.*, *55*, 246–255 (1977).

21. S. J. Kim, "Factors Influencing Colloidal Particle Transport in Porous Media," Ph.D. Dissertation, Auburn University, Auburn, AL, 1993.
22. D. Chan and D. J. Mitchell, "The Free Energy of an Electrical Double Layer," *J. Colloid Interface Sci.*, *95*, 193–197 (1983).
23. D. Chan, J. W. Perram, L. R. White, and T. W. Healy, "Regulation of Surface Potential at Amphoteric Surfaces during Particle–Particle Interaction," *J. Chem. Soc., Faraday Trans. I*, *71*, 1046–1057 (1975).
24. J. Gregory, "Interfacial Phenomena," in *The Scientific Basis of Filtration* (K. J. Ives, Ed.), Noordhoff International Publishing, Leyden, Netherlands, 1975.
25. H. Hohl, L. Sigg, and W. Stumm, "Characterization of Surface Chemical Properties of Oxides in Natural Waters: The Role of Specific Adsorption in Determining the Surface Charge," in *Particulates in Water* (Advances in Chemistry Series 189, M. C. Kavanaugh and J. O. Leckie, Eds.), American Chemical Society, 1980, pp. 1–32.
26. R. J. Hunter, *Zeta Potential in Colloid Science: Principles and Applications*, Academic Press, London, 1981.
27. P. C. Hiemenz, *Principles of Colloid and Surface Chemistry*, Dekker, New York, NY, 1977.
28. E. J. W. Verwey and J. Th. G. Overbeek, *Theory of the Stability of Lyophobic Colloids: The Interaction of Sol Particles Having an Electric Double Layer*, Elsevier, New York, NY, 1948.
29. J. Czarnecki and T. Dabroś, "Attenuation of the van der Waals Attraction Energy in the Particle/Semi-Infinite Medium System Due to the Roughness of the Particle Surface," *J. Colloid Interface Sci.*, *78*, 25–30 (1980).
30. J. Czarnecki and V. Itschenskij, "van der Waals Attraction Energy between Unequal Rough Spherical Particles," *Ibid.*, *98*, 590–591 (1984).
31. J. Czarnecki, "The Effects of Surface Inhomogeneities on the Interactions in Colloidal Systems and Colloid Stability," *Adv. Colloid Interface Sci.*, *24*, 283–319 (1986).
32. Z. Adamczyk, M. Zembala, B. Siwek, and J. Czarnecki, "Kinetics of Latex Particle Deposition from Flowing Suspensions," *J. Colloid Interface Sci.*, *110*, 188–200 (1986).
33. S. S. Dukhin and J. Lyklema, "Dynamics of Colloid Particle Interaction," *Langmuir*, *3*, 94–98 (1987).
34. H. P. van Leeuwen and J. Lyklema, "Interfacial Electrodynamics of Interacting Colloidal Particles. Geometrical Aspects," *Ber. Bunsenges. Phys. Chem.*, *91*, 288–291 (1987).
35. C. R. O'Melia, "Particles, Pretreatment, and Performance in Water Filtration," *J. Environ. Eng.*, *111*, 874–890 (1985).
36. R. Rajagopalan and J. S. Kim, "Adsorption of Brownian Particles in the Presence of Potential Barriers: Effect of Different Modes of Double-Layer Interaction," *J. Colloid Interface Sci.*, *83*, 428–448 (1981).
37. J. Th. G. Overbeek, "Electrochemistry of the Double Layer," in *Colloid Science: Irreversible Systems* (H. R. Kruyt, Ed.), Elsevier, Amsterdam, 1952.
38. D. C. Prieve and E. Ruckenstein, "Role of Surface Chemistry in Particle Deposition," *J. Colloid Interface Sci.*, *60*, 337–348 (1977).
39. K. M. Yao, M. T. Habibian, and C. R. O'Melia, "Water and Waste Water Filtration: Concepts and Applications," *Environ. Sci. Technol.*, *5*, 1105–1112 (1971).
40. L. A. Spielman, "Particle Capture from Low-Speed Laminar Flows," *Annu. Rev. Fluid Mech.*, *9*, 297–319 (1977).
41. R. Rajagopalan and C. Tien, "Experimental Analysis of Particle Deposition on Single Collectors," *Can. J. Chem. Eng.*, *55*, 256–264 (1977).
42. J. A. Fitzpatrick and L. A. Spielman, "Filtration of Aqueous Latex Suspensions through Beds of Glass Spheres," *J. Colloid Interface Sci.*, *43*, 350–369 (1973).

Received by editor January 8, 1996